J Mater Sci (2016) 51:8442–8451

Redox-responsive biodegradable nanogels for photodynamic therapy using Chlorin e6

Hyoyong Kim[1], Byoungjae Kim[1], Chaeyeon Lee[1], Jung Lim Ryu[2], Seong-Jin Hong[2], Jinku Kim[3], Eun-Ju Ha[1,*], and Hyun-jong Paik[1,*]

[1] *Department of Polymer Science and Engineering, Pusan National University, Busan 609-735, Korea*
[2] *Center of Photodynamic Therapy (PDT), Diatech Korea Co., Ltd, Songpa-gu, Seoul 138-826, Korea*
[3] *Department of Bio and Chemical Engineering, Hongik University, Sejong 339-701, Korea*

Received: 22 February 2016
Accepted: 26 May 2016
Published online: 8 June 2016

ABSTRACT

Recent advances in drug carrier design in the field of photodynamic therapy (PDT) have stimulated the development of numerous sophisticated drug delivery carriers. We developed novel biodegradable and biocompatible nanogels as PDT carriers. The nanogels were synthesized by ATRP technique using inverse miniemulsion and their biodegradability was determined in the presence of glutathione. The model photosensitizer (PS) was encapsulated in the biodegradable nanogels by simple mixing and sonication. The cellular uptake of the PS-loaded nanogels and the cytotoxicity of the nanogels before and after laser irradiation were determined using HeLa cells. The results showed that the Ce6-nanogel complex was well internalized into the tumor cells, and the Ce6-loaded nanogels did not influence on cellular viability of the cells before light irradiation. Under light exposure, however, the Ce6-nanogel complex-treated HeLa cells revealed strong photoactivity. These nanogels may enhance therapeutic efficacy of PSs without any complex chemical modifications with PSs.

Introduction

Photodynamic therapy (PDT) is one of the most promising treatments for various diseases such as tumors. It is a non-invasive method using photosensitizers (PSs) and reactive oxygen species (ROS) under light of appropriate wavelength [1–3]. When PSs are combined with harmless visible light of defined wavelength, which excites the PSs to a high energy triplet state, the PSs react with cellular oxygen to form toxic reactive oxygen species (ROS) such as singlet oxygen and oxygen radicals [4, 5]. ROS can oxidize cellular nucleic, fatty, and amino acids, and ultimately induce cell death [6].

However, PSs have some drawbacks such as low solubility in water (hydrophobicity) and non-specific distribution after intravenous injection [7, 8]. Thus, they are apt to aggregate under physiological conditions, significantly reducing the quantum yields of ROS production. Even in the case of water-soluble PSs, the selective accumulation at malignant site is not high enough for clinical use [9]. In this respect,

Address correspondence to E-mail: eunju0916@gmail.com; hpaik@pusan.ac.kr

DOI 10.1007/s10853-016-0104-4

the incorporation of PSs into water-dispersible nanocarriers, so-called "nanophotosensitizers (NPSs)," can enhance the solubility of PSs as well as the selectivity of the treatment by efficient intracellular delivery of the PS payload, with or without active targeting moieties such as proteins, peptides, and aptamers [10]. Unlike typical drug delivery systems, NPSs do not need to release the PS molecules, instead, it is essential that ROS can diffuse in and out of the nanoparticle matrices to exert therapeutic efficacy by photosensitization.

PDT carriers must fulfill several requirements: (1) minimal internal toxicity, (2) tumor selectivity and adequate retention ability, (3) sufficient encapsulation capacity and rapid release property, and (4) protection of the PSs from enzymatic or biological degradation.

There are numerous candidates satisfying above requirements such as liposome, polymeric micelles, organic/inorganic nanoparticles, and nanogels [11]. Among candidates, nanogels attract substantial interest of many research groups. Nanogels are composed of water-soluble monomer and cross-linked by various cross-linkers [12]. The size of nanogels can be easily controlled by synthesis methods and the dimension of nanogels is very stable in normal condition; thus, the encapsulated drug cannot be released. Moreover, fascinating class of nanomaterials have emerged for highly sophisticated delivery systems, which contain stimuli-responsive functional groups for releasing loaded drugs such as disulfide linkage (reduction responsive), orthoester (pH responsive), or LCST polymers (temperature responsive) [13, 14].

Among various types of nanogels, biodegradable, well-defined, and water-dispersible nanogels have been synthesized using ATRP techniques in an inverse miniemulsion [15, 16]. These nanogels can produce a number of attractive features for PDT carriers. For example, the resulting nanogels could be readily functionalized with biomolecules by utilizing halide end-functionality [17–19]. In addition, individual nanogels with uniformly cross-linked network enable to control the release of encapsulated therapeutic agents [20, 21]. Furthermore, nanogel-based delivery system increase blood circulation time of the encapsulated PDT before degradation and will be easily cleared by the RES (reticuloendothelial system) upon degradation [22].

As a step toward to demonstrate the usefulness of nanogels for PDT nanocarriers, in this study, we report the potential of the nanogels as a PDT carrier. The well-defined biodegradable nanogels were synthesized by ATRP in inverse miniemulsion and the biodegradability of the nanogels cross-linked with disulfide bonds was determined in the presence of glutathione (GSH). The PS molecule, chlorin e6 (Ce6), for PDT was encapsulated into the nanogels by sonication and the encapsulation efficiency was determined by UV–Vis absorbance spectra. The in vitro cellular uptake and phototoxicity of the encapsulated PS in the nanogels were determined using human cervical cancer cells (HeLa cells).

Experimental

Materials

Oligo(ethylene glycol) monomethyl ether methacrylate with $M_n = 300$ g/mol and pendent EO units DP $\gg 5$ (OEOMA, Aldrich) was purified by passage through a column filled with basic alumina to remove inhibitor. Copper(II)bromide ($CuBr_2$, 99 %), L-ascorbic acid (AscA, 99 + %) and glutathione (GSH, 98 %) from Aldrich, sorbitan monooleate (Span 80, YAKURI), tetrahydrofuran (THF, extra pure grade, SAMCHUN), and cyclohexane (extra pure grade, KANTO) were used as received. Chlorin e6 (Ce6) was provided by Diatech Korea Co., Ltd. (Songpa-Gu, Seoul, Korea). Tris[(2-pyridyl)methyl]amine (TPMA), dithiopropionyl poly(ethylene glycol) dimethacrylate (ssDMA), and poly(ethylene oxide) (PEO)-functionalized bromoisobutyrate (PEO5000-Br, pendent EO units DP 113) were synthesized and purified as described elsewhere.

Measurement

^{1}H-NMR spectra were recorded using a 500 MHz Varian spectrometer. Dynamic light scattering (DLS) studies were performed with a 90 Plus Particle Size Analyzer from Brookhaven Instruments Corporation. Non-contact (tapping) AFM was performed with an n-Tracer SPM (Nanofocus). The cantilever was composed of silicon and had a resonance frequency of approximately 320 kHz and a nominal radius of curvature of less than 8 nm. The images were obtained at room temperature in air. Molecular

weights (M_n) and molecular weight distributions (M_w/M_n) were determined using gel permeation chromatography (GPC) after calibration with polystyrene standards. GPC was equipped with Agilent 1100 pump, RID detector, and PSS SDV (5 μm, 10^5, 10^3, 10^2 Å, 8.0 × 300.0 mm) columns. The fluorescent images of Ce6-loaded nanogels were measured by Leica TCS SP8 STED. The capacity of encapsulated Ce6 was measured by Optizen 3220UV UV–Vis spectroscopy. The encapsulation of Ce6 in the nanogels was confirmed by photoluminescent spectroscopy. FT-IR spectra of all the samples were taken on an Agilent Technologies Cary 600 Series spectrometer using KBr pellets. The cell viability assay was carried out with LATUS-PDT (LATUS 2.662.4) as a laser medical apparatus.

Synthesis of poly(ethylene glycol)-functionalized bromoisobutyrate (PEO5000-Br) macroinitiator

A water-soluble macroinitiator, poly(ethylene glycol) (PEO)-functionalized bromoisobutyrate (PEO5000-Br), was synthesized using a reported procedure. Poly(ethylene glycol) monomethyl ether (PEO5000-OH, $M = 5000$ g/mol, 5.0 g, 1.0 mmol) was reacted with 2-bromoisobutyryl bromide (0.46 g, 2.0 mmol) in the presence of triethylamine (0.2 g, 2.0 mmol) in dichloromethane (75 mL). The product was mixed with Hexane, isolated from dispersion by vacuum filtration, and then dried in a vacuum oven at 25 °C for 24 h. In this way, residues could be removed from the final product. ^{1}H-NMR (CDCl3): 1.9 [s, 6H, –C(CH_3)$_2$Br], 3.3 (s, 3H, –OCH_3), 3.35–3.8 (m, EO protons), 4.2 [m, 2H, –CH_2–O(O)C].

Synthesis of dithiopropionyl poly(ethylene glycol) dimethacrylate (ssDMA)

Poly(ethylene glycol) methacrylate (PEOMA500, $M = 500$ g/mol) was purified using the solvent extraction method as described elsewhere. A solution consisting of dithiopropionic acid (2.3 g, 10.0 mmol) in dried THF (15 ml) was added dropwise to a solution consisting of the purified PEOMA500 (9.5 g, 19.0 mmol), DCC (3.9 g, 19.0 mmol), and a catalytic amount of DMAP (0.5 g, 2.14 mmol), in dichloromethane (30 ml) in an ice bath at 0 °C for 20 min. The resulting mixture was allowed to stir at room temperature for 12 h. The formed solids were removed by vacuum filtration and the combined solvents were removed by rotary evaporation. The resulting oily residue was dissolved in dichloromethane (100 ml), and was washed with aqueous $NaHCO_3$ solution three times to remove excess diacid. After dichloromethane was removed, the resulting yellow oily residue was dissolved in a minimum amount of THF (5 ml), and put in refrigerator at −5 °C for 12 h. The insoluble solids were removed by vacuum filtration, THF was removed by rotary evaporation, and then the product was dried in a vacuum oven at 35 °C for 12 h. ^{1}H-NMR (DMSO-d_6): 1.9 (s, 6H, CH_3–), 2.7 [t, 4H, –C(O)–CH_2–CH_2–SS–], 2.9 [t, 4H, –O(O)C–CH_2–CH_2–SS–], 3.3–3.7 [m, 72H, –(CH_2CH_2O)n–], 4.0–4.3 [m, 8H, –C(O)O–CH_2– and –CH_2–O(O)C–], 5.7 (s, 2H, CH=), 6.0 (s, 2H, CH=).

Synthesis of nanogels using AGET ATRP in inverse miniemulsion

Following a procedure similar to a previous report [16], uniform and stable cross-linked nanogels were prepared by AGET atom-transfer radical polymerization (ATRP) of OEOMA300 in inverse miniemulsion in the presence of ssDMA as degradable cross-linkers. Typical procedure for the synthesis of biodegradable nanogels follows: OEOMA300 (1.3 g, 4.3 mol), PEO5000-Br (74 mg, 0.014 mol), TPMA (2.0 mg, 0.007 mol), $CuBr_2$ (1.6 mg, 0.007 mol), ssDMA (153 mg, 0.13 mol), and water (1.4 mL) were mixed in a 50-mL vial at room temperature. The resulting clear solution was mixed with a solution of Span 80 (1.0 g) in cyclohexane (20 g), and the mixture was sonicated for 2 min in an ice bath at 0 °C to form a stable inverse miniemulsion. The dispersion was transferred into a 50-mL Schlenk flask, and then bubbled with nitrogen for 30 min. The flask was immersed in an oil bath preheated to 30 °C, and then an N_2-purged aqueous solution of ascorbic acid (0.028 mmol/mL, 0.004 mmol, 155 μL) was added via syringe to start the polymerization. The polymerization was stopped by exposing the reaction mixture to air. The resulting nanogels were purified by removal of the cyclohexane, addition of THF, and then the resulting heterogeneous mixture was stirred at room temperature for 5 h. The gels were separated by centrifugation (15000 rpm × 20 min) and decantation of the supernatant. THF was added and the same procedure was repeated twice to remove THF-soluble species such as unreacted monomers

and Span 80 (surfactant). After the final wash, the precipitate was dried in a vacuum oven at 30 °C for 2 h to yield nanogels.

Degradation of nanogels in glutathione

Cross-linked nanogels were degraded into the corresponding linear polymers in the presence of aqueous GSH solution at room temperature. Typically, purified, dried nanogels (15.0 mg, 0.001 mol—disulfide linkage) were stirred in deionized water (5 mL) at room temperature for 24 h to allow the nanogels to be fully hydrated. Excess GSH (15.0 mg, 0.05 mol) was added under N_2 atmosphere for protecting oxidation of thiol groups and the reaction mixture was stirred for 3 days. After degradation was completed, an aliquot of the mixture was taken, dried, and analyzed by GPC and DLS.

Preparation of Ce6-loaded nanogels

Dried nanogels (30 mg) were stirred in THF (10 mL) for 24 h to allow the nanogels to be fully hydrated, and subsequently, hydrated nanogels were mixed with Ce6 solution (THF 1.5 mL, 0.2 mg/mL). The mixture was sonicated for 30 min, and then purified by the same method used for nanogel purification mentioned above. Using supernatant, encapsulation efficiency was calculated by UV–Vis absorbance spectra. After removing free Ce6, Ce6-loaded nanogels were transferred to a dialysis bag with a membrane cutoff size of 12–14 kDa. The mixture was dialyzed against water for 3 days, during which the water was changed 5 times.

Cellular uptake assay

For in vitro cellular assays, the HeLa cells, which were derived from human cervical cancer, were cultured at 37 °C with 5 % CO_2 atmosphere in DMEM (HyClone) containing 10 % fetal bovine serum (Hyclone) and 1 % penicillin/streptomycin (Hyclone). The cells were allowed to grow until they reached 80 % confluence and then were subcultured. The 3–5 passage number cells were used in this assay. In a 6 well plate, HeLa cells (1×10^5/well) were seeded and incubated for 48 h. After 48 h, the HeLa cells were treated 5 μM drug and incubated for 3, 5, and 7 h, respectively. After each time period, treated drug was washed twice with PBS and then fluorescence images were obtained.

In vitro photoactivity assay

Cell viability was assessed in a WST (water-soluble tetrazolium salt) assay using the EZ-Cytox kit. HeLa cells (1×10^4/200 μL/well) were seeded in a 96-well microplate, and incubated for 24 h. Subsequently, the medium on the cell was replaced with fresh medium Ce6-loaded nanogels and the cells were incubated for another 3 h. The cells were then irradiated with a laser at 660 ± 5 nm (12.5 J/cm^2) on a 96-well plate and incubated to stabilize for 20 min. The treated drug was removed and the cells were washed with a PBS. The concentrations of remaining viable cells were determined by the EZ-cytox kit (WST assay). For the WST assay, 10x diluted EZ-cytox kit solution was treated into the each well. After 3 h, the absorbance at 450 nm was measured using a microplate reader.

Results and discussion

Synthesis and characterization of biodegradable nanogels

The formation of uniformly cross-linked nanogels with controlled molecular weight and molecular weight distribution is possible under inverse miniemulsion ATRP [16]. The nanogels containing disulfide group in the backbone is degraded under reducing atmosphere such as GSH. Therefore, the synthesized nanogels encounter GSH in the body, and they are degraded into corresponding linear polymers with appropriate molecular weight, which can be filtered in kidney.

Biodegradable nanogels were synthesized by inverse miniemulsion ATRP as shown in Scheme 1. The size and size distribution of the synthesized biodegradable nanogels were measured in cyclohexane before purification. As shown in Fig. 1, the synthesized particles are polymerized into nanogels of a uniform size of approximately 247–254 nm, with a narrow size distribution (standard deviation of 3.5 nm). The particles did not dissolve in any solvent, including THF or water, indicating that the particles had cross-linked network during polymerization. The morphology of biodegradable nanogels was analyzed

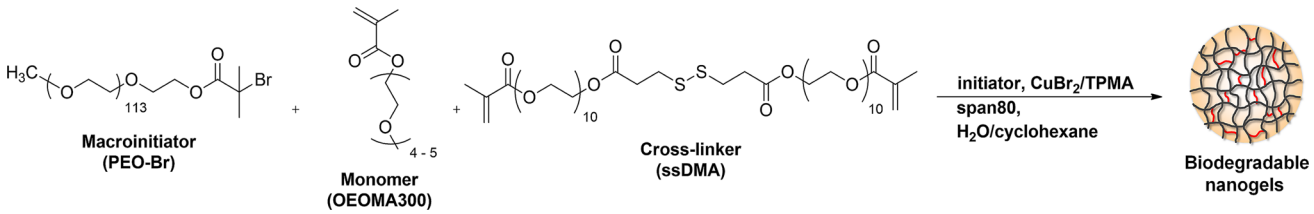

Scheme 1 Synthesis scheme of biodegradable nanogels by inverse miniemulsion ATRP.

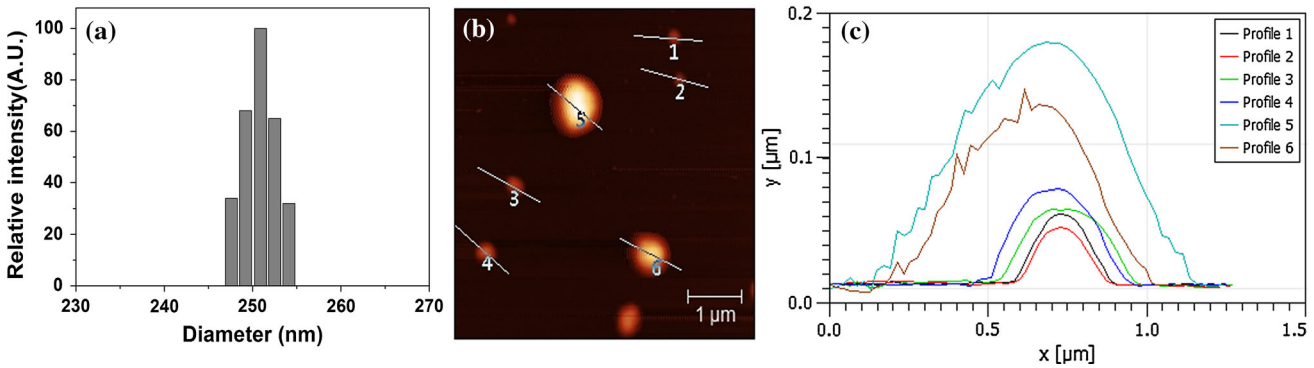

Figure 1 Size distribution of nanogels in cyclohexane was measured by DLS (**a**), morphology of biodegradable nanogels on mica surface analyzed by tapping mode AFM (**b**), and each height profile of nanogels (**c**).

by tapping mode AFM. Figure 1 shows the AFM images of biodegradable nanogels on mica surface b and height profile of nanogels c. Biodegradable nanogels were mixed with small amount of larger particles which suggested the formation of aggregates during polymerization. The average diameter is larger than DLS measurement because of flattening of the nanogels on the mica surface during casting process and aggregation of the nanogels. The height of nanogels represents that the particles were cross-linked by ssDMA. Uncross-linked particles show lower height because it cannot maintain the spherical shape [16]. As seen in Fig. 2, the FT-IR spectra of the OEOMA and ssDMA exhibit two characteristic bands at 1640 cm^{-1} corresponding to C=C and 1720 cm^{-1} C=O vibrational absorption. The absorption peak of the nanogel at 1640 cm^{-1} in FT-IR spectrum was disappeared, which confirmed the formation of the biodegradable nanogels.

Degradation study of nanogels

Drug carriers for proper distribution of drug to proper organ or site of disease must be removed after the end of the treatment. If not, they can cause various side effects such as inflammation. Thus, we designed the nanogels for PS carrier using biocompatible monomer and biodegradable crosslinker. The synthesized nanogels were cross-linked by ssDMA, which is composed of disulfide linkage. Disulfide group can be reduced by thiol group such as GSH in the body [23–28].

To determine biodegradability, synthesized nanogels were mixed with GSH solution. After 3 days, the size of the degradation products in the solution was measured by DLS, and it was about 50 nm (Fig. 3a), which was much smaller than the original nanogel size. The molecular weight of the degraded polymer was 25140 g/mole, measured by GPC, and its molecular weight distribution was 1.38 (Fig. 3b). The turbidity of the solution after degradation was decreased as compared to before degradation, indicating that the particles in the solution before degradation were much smaller than before the degradation, probably because the particle size is not enough to scatter the light. (Figure 3b)

Loading of Ce6 into biodegradable nanogels

Chlorin e6 (Ce6) is a photosensitizer widely used for the treatment of various cancers [9]. In this study, biodegradable nanogels were designed for passive

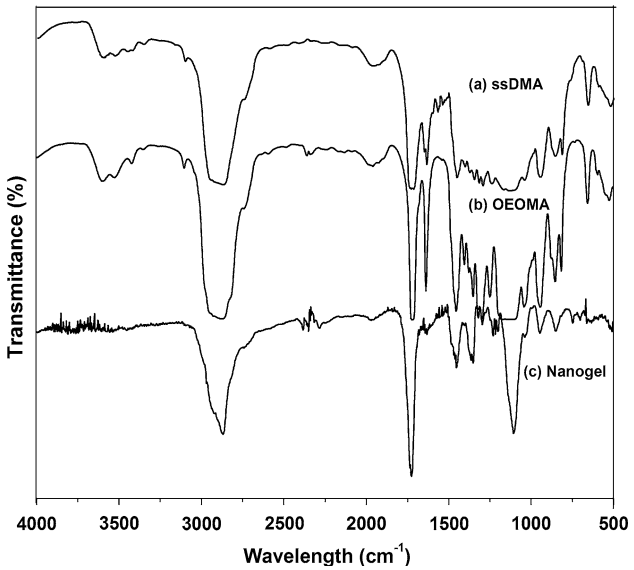

Figure 2 FT-IR spectra of ssDMA (*a*), OEOMA (*b*), and biodegradable nanogels (*c*).

targeting to tumor tissues. The nanogels were mixed with Ce6 (200 μg) in THF and then Ce6-loaded nanogels were readily prepared by sonication for 30 min. After sonication, Ce6-loaded nanogels and free Ce6 were separated by centrifugation and the supernatant was used for measurement of UV–Vis absorbance. The absorbance of three different concentrations of Ce6 (3.3, 6.6, 13.2 μg/mL in THF) was measured to confirm extinction coefficient, and the calibration curve was obtained after measuring the absorbance of different concentrations which is 668 nm. The absorbance of the supernatant of centrifuged Ce6-loaded nanogels was measured with UV–Vis spectrometer to confirm unloaded Ce6 (Fig. 4). The amount of Ce6 in nanogels was 86 μg. Drug loading efficiency of nanogels was approximately 43 wt% and drug loading capacity of dry nanogels was calculated to 2.5 %.

Their light emission spectra at 668 nm were determined and the Ce6 encapsulated in the nanogels showed much higher photoluminescence than the Ce6 solution alone (Fig. 5). The data showed that Ce6-loaded nanogels exhibited much more emission intensity between 600 and 700 nm, compared to free Ce6. In general, Ce6 can aggregate in aqueous media due to the hydrophobic and π–π interactions of the PS, resulting in the decrease of its photoactivity [29, 30]. However, in this system, Ce6 has been physically entrapped in amphiphilic nanogels based on Poly(ethylene glycol) methacrylate by hydrophobic interactions [31]. Thus, the increased intensity of photoluminescence indicates that Ce6 molecules encapsulated in nanogels were well dispersed in the media, leading to much greater photoactivity of the PS molecule, compared with Ce6 alone. Therefore, it is likely to assume that the aggregation behavior was eliminated due to improved solvent-dispersibility of Ce6 molecules resulting from the amphiphilicity of the nanogels [29–36]. This is encouraging since simple mixing of the PS with the nanogels without any further functionalization yields dramatic increase of photoluminescence of the molecule. Therefore, the nanogels used in the study may be an excellent choice as PS carriers as compared to other sophisticated carriers, whose syntheses often require complex chemistries and multiple synthesis steps. And the fluorescent of Ce6-loaded nanogels was taken by fluorescent microscopy. As shown in Fig. 6, red

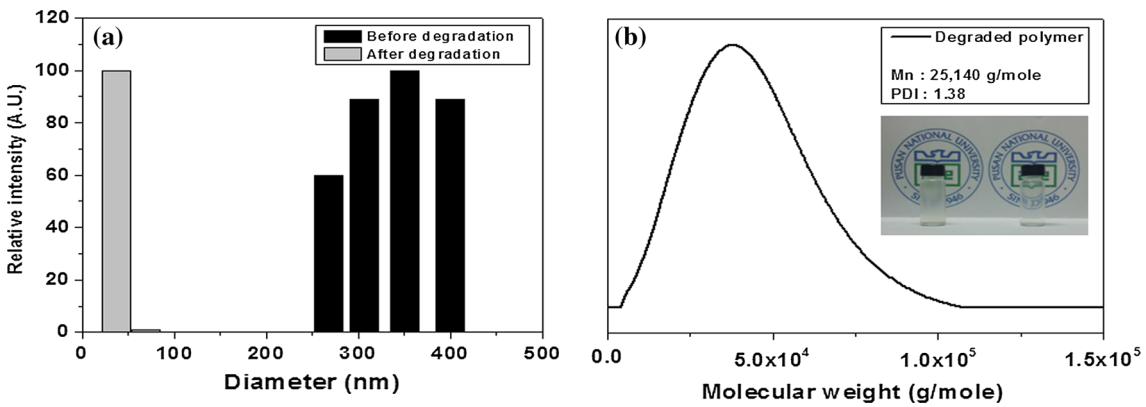

Figure 3 **a** The hydrodynamic size of nanogels before and after degradation in the presence of glutathione (GSH) was measured by DLS. **b** GPC trace of degraded nanogel. *The inset* is photograph of biodegradable nanogels, before (*left*) and after (*right*) degradation.

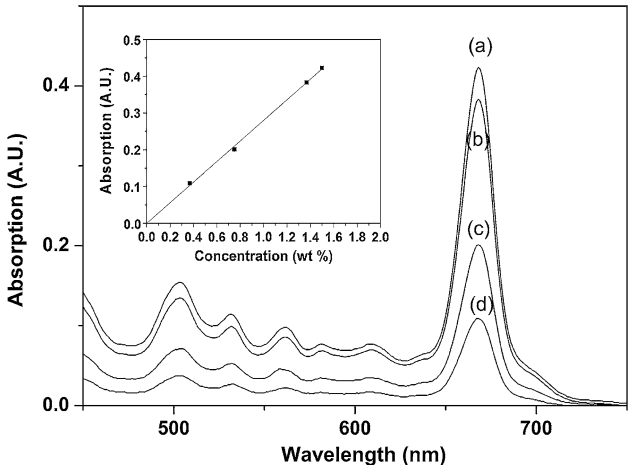

Figure 4 Absorption spectra of free Ce6 solutions at different concentrations: (*a*) 13.2 (*c*) 6.6 (*d*) 3.3 μg/mL and (*b*) unloaded Ce6 solution. *The inset* shows the concentration dependence of the absorbance of Chlorin e6 solutions at 668 nm.

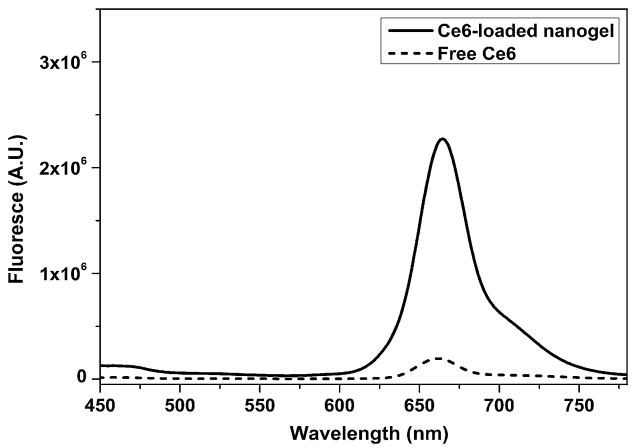

Figure 5 Fluorescent spectra of free Chlorin e6 and Chlorin e6-loaded nanogels in THF.

fluorescent represents the encapsulation of Ce6 in biodegradable nanogels.

In vitro cellular uptake of Chlorin e6-loaded nanogels

The in vitro cellular uptake of Ce6-loaded nanogel in HeLa cells was evaluated by fluorescence microscopy (Fig. 7). Ce6 is visualized with red fluorescence through Cy5 filter lens, and the data indicate that Ce6-loaded nanogels are localized inside the cell via endocytosis. HeLa cells incubated with Ce6-loaded nanogels for 3 h showed the strongest red fluorescence, compared to later time points. These data indicate that the molecules were released from the

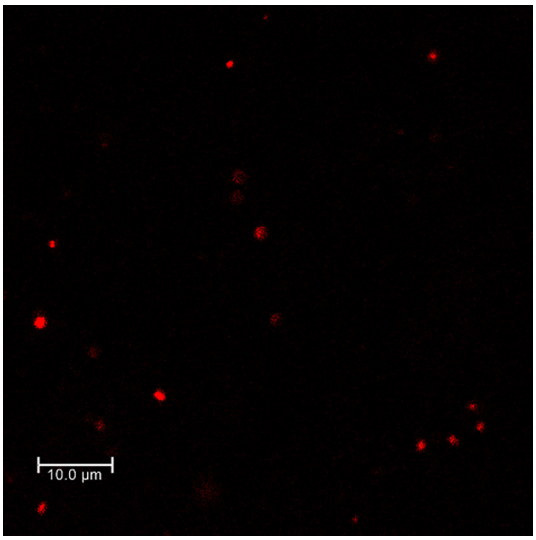

Fig. 6 Fluorescent image of Ce6-loaded nanogels. *Red fluorescent* represents Ce6 were successfully encapsulated in biodegradable nanogels.

cells over time, which is critical to enhance therapeutic efficacy of PSs [26].

PDT effect on in vitro cell viability

To assess the cytotoxicity of Ce6-loaded nanogels, the cell viability of HeLa cells incubated with Ce6-loaded nanogels (3, 4, and 7 μM) for 3 h was determined using the EZ-Cytox kit. The data revealed that cell viabilities at any concentrations without light exposure were over 90 %, implying that the presence of Ce6-loaded nanogels in the cells did not influence cell viability (Fig. 8). However, when HeLa cells with Ce6-loaded nanogels were irradiated to laser for 400 s, the viabilities of the cells showed the concentration-dependent phototoxicity, where the viabilities were less than 40 % for 2.5 μM and more than 90 % for 3.5 and 4 μM.

Overall, the data demonstrate the potential of the nanogels as hydrophobic drug carriers without substantial cytotoxicity. In addition, the nanogels combined with PSs can be used for PDT, which may selectively target the tumor cells using light irradiation.

Conclusions

Biodegradable and biocompatible nanogels were synthesized by inverse miniemulsion ATRP for PDT drug carrier and their biodegradability was

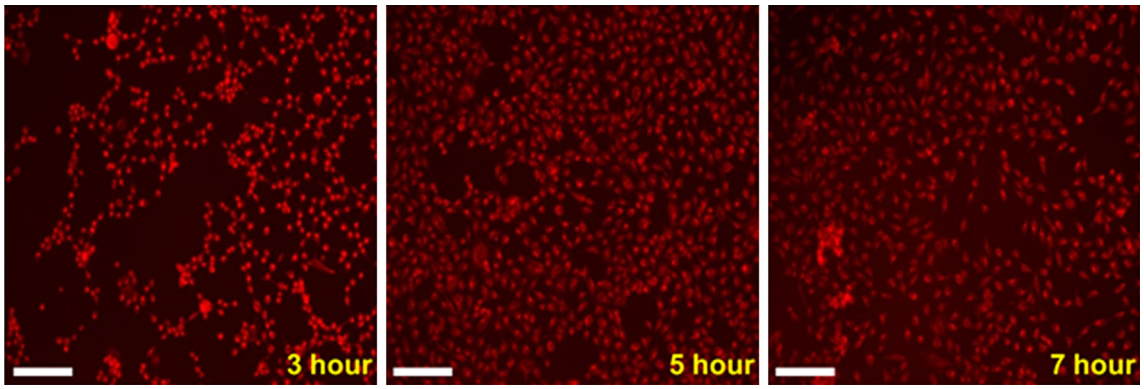

Figure 7 Fluorescent images of HeLa cells with Ce6-loaded nanogels as a function of incubation time (*scale bar* 300 μm).

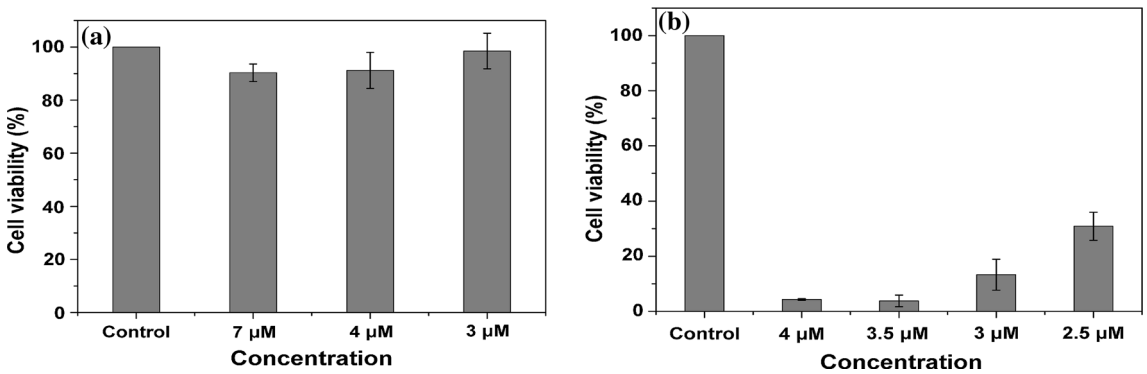

Figure 8 In vitro cell viability of HeLa cells upon treatment with different concentrations of Ce6-loaded nanogels in the (**a**) absence and (**b**) presence of laser irradiation.

confirmed in GSH degradation studies. Ce6, an insoluble PSs, was easily encapsulated in these biodegradable nanogels by sonication. The Ce6-loaded nanogels were readily internalized into HeLa cells and the Ce6-loaded nanogels did not exhibit any cell toxicity in the absence of laser irradiation. However, the Ce6-loaded nanogels under laser exposure showed strong photoactivity on the cells. The nanogels may be useful as nanophotosensitizers (NPSs), which can enhance the solubility of PSs and intracellular delivery of the PS payload.

Acknowledgements

This work was supported by the Basic Science Research Program through the National Research Foundation of Korea (NRF) grant funded by the Korea government (MSIP) (2013R1A2A2A01068818); the National Research Foundation of Korea NRF—2014R1A1A2008659; and the National Research Foundation of Korea (NRF) funded by the Ministry of Education (2013R1A1A4A010101185). The authors also acknowledge the Korea Basic Science Institute for assistance with the FT-NMR spectrometer.

References

[1] Wang SZ, Gao RM, Zhou FM, Selke M (2004) Nanomaterials and singlet oxygen photosensitizers: potential applications in photodynamic therapy. J Mater Chem 14:487–493

[2] Jang B, Park JY, Tung CH, Kim IH, Choi Y (2011) Gold nanorod-photosensitizer complex for near-infrared fluorescence imaging and photodynamic/photothermal therapy in vivo. ACS Nano 5(2):1086–1094

[3] Chatterjee DK, Fong LS, Zhang Y (2008) Nanoparticles in photodynamic therapy: an emerging paradigm. Adv Drug Deliv Rev 60(15):1627–1637

[4] Celli JP, Spring BQ, Rizvi I et al (2010) Imaging and photodynamic therapy: mechanisms, monitoring, and optimization. Chem Rev 110(5):2795–2838

[5] DeRosa MC, Crutchley RJ (2002) Photosensitized singlet oxygen and its applications. Coord Chem Rev 233–234:351–371

[6] Triesscheijin M, Baas P, Schellens JH, Stewart FA (2006) Photodynamic therapy in oncology. Oncologist 11(9): 1034–1044

[7] Lee DJ, Youn YS, Lee ES (2015) Photodynamic tumor therapy of nanoparticles with chlorin e6 sown in poly (ethylene glycol) forester. J Mater Chem B 3:4690–4697

[8] Lam KS, Li YP, Lin TY et al (2013) Novel multifunctional nanocarriers for drug delivery, photodynamic therapy, sonodynamic therapy, MRI and PET imaging. Cancer Res 73:4508

[9] Konan YN, Gurny R, Allemann E (2002) State of the art in the delivery of photosensitizers for photodynamic therapy. J Photochem Photobiol 66(2):89–106

[10] Huang X, EI-Sayed IH, Qian W, EI-Sayed MA (2006) Cancer cell imaging and photothermal therapy in the near-infrared region by using gold nanorods. J Am Chem Soc 128(6):2115–2120

[11] Peer D, Karp JM, Hong S, FaroKHzad OC, Margalit R, Langer R (2007) Nanocarriers as an emerging platform for cancer therapy. Nat Nanotechnol 12:751–760

[12] Chacko RT, Ventura J, Zhuang JM, Thayumanavan S (2012) Polymer nanogels: a versatile nanoscopic drug delivery platform. Adv Drug Deliv Rev 64(9):836–851

[13] Meng FH, Hennink WE, Zhong Z (2009) Reduction-sensitive polymers and bioconjugates for biomedical applications. Biomaterials 30(12):2180–2198

[14] Zhang Q, Ko NR, Oh JK (2012) Recent advances in stimuli-responsive degradable block copolymer micelles: synthesis and controlled drug delivery applications. Chem Commun 48(61):7542–7552

[15] Oh JK, Siegwart DJ, Lee H-I et al (2007) Biodegradable nanogels prepared by atom transfer radical polymerization as potential drug delivery carriers: synthesis, biodegradation, in vitro release, and bioconjugation. J Am Chem Soc 129(18):5939–5945

[16] Oh JK, Tang C, Gao H, Tsarevsky NV, Matyjaszewaki K (2006) Inverse miniemulsion ATRP: a new method for synthesis and functionalization of well-defined water-soluble/cross-linked polymeric particles. J Am Chem Soc 128(16):5578–5584

[17] Hawker CJ, Wooley KL (2005) The convergence of synthetic organic and polymer chemistries. Science 309(5738):1200–1205

[18] Gao HF, Louche G, Sumerlin BS, Jahed N, Golas P, Matyjaszewaki K (2005) Gradient polymer elution chromatographic analysis of α, ω-dihydroxypolystyrene synthesized via ATRP and click chemistry. Macromolecules 38(22):8979–8982

[19] Lutz JF, Borner HG, Weichenhan K (2006) Combining ATRP and "click" chemistry: a promising platform toward functional biocompatible polymers and polymer bioconjugates. Macromolecules 399(19):6376–6383

[20] Eichenbaum KD, Thomas AA, Eichenbaum GM, Gibney BR, Needham D, Kiser PF (2005) Oligo-α-hydroxy ester cross-linkers: impact of cross-linker structure on biodegradable hydrogel networks. Macromolecules 38(26): 10757–10762

[21] Huang X, Lowe TL (2005) Biodegradable thermoresponsive hydrogels for aqueous encapsulation and controlled release of hydrophilic model drugs. Biomacromolecules 6(4): 2131–2139

[22] Seymour LW, Duncan R, Strohalm J, Kopecek J (1987) Effect of molecular weight (M_w) of *N*-(2-hydroxypropyl)methacrylamide copolymers on body distribution and rate of excretion after subcutaneous, intraperitoneal, and intravenous administration to rats. J Biomed Mater Res 21(11):1341–1358

[23] Tsarevsky NV, Sarbu T, Goebelt B, Matyjaszewski K (2002) Synthesis of styrene-acrylonitrile copolymers and related block copolymers by atom transfer radical polymerization. Macromolecules 35:6142–6148

[24] Kim H, Mun S, Choi Y (2013) Photosensitizer-conjugated polymeric nanoparticles for redox-responsive fluorescence imaging and photodynamic therapy. J Mater Chem B 1:429–431

[25] Cheng R, Feng F, Meng F, Deng C, Feujen J, Zhong Z (2011) Glutathione-responsive nano-vehicles as a promising platform for targeted intracellular drug and gene delivery. J Control Release 152:2–12

[26] Pan Y-J, Chen Y-Y, Wang D-R, Wei C, Guo J, Lu D-R, Chu C-C, Wang C-C (2012) Redox/Ph dual stimuli-responsive biodegradable nanohydrogels with varying responses to dithiothreitol and glutathione for controlled drug release. Biomaterials 33:6570–6579

[27] Ding J, Shi F, Xiao C, Lin L, Chen L, He C, Zhuang X, Chen X (2011) One-step preparation of reduction-responsive poly(ethylene glycol)-poly(amino acid)s nanogels as efficient intracellular drug delivery platforms. Polym Chem 2:2857–2864

[28] Saito G, Swanson JA, Lee KD (2003) Drug delivery strategy utilizing conjugation via reversible disulfide linkages: role and site of cellular reducing activities. Adv Drug Deliv Rev 55(2):199–215

[29] Park W, S-j Park, Na K (2011) The controlled photoactivity of nanoparticles derived from ionic interactions between a

water soluble polymeric photosensitizer and polysaccharide quencher. Biomaterials 32:8261–8270

[30] Park H, Na K (2013) Conjugation of the photosensitizer Chlorin e6 to Pluronic F127 for enhanced cellular internalization for photodynamic therapy. Biomaterials 34:6992–7000

[31] Oh JK, Siegwart DJ, Lee H-I, Sherwood G, Peteanu L, Hollinger JO, Kataoka K, Matyjaszewski K (2007) Biodegradable nanogels prepared by atom transfer radical polymerization as potential drug delivery carriers: synthesis, biodegradation, in vitro release, and bioconjugation. J Am Chem Soc 129:5939–5945

[32] Zhang D, Wu M, Zeng Y, Wu L, Wang Q, Han X, Liu X, Liu J (2015) Chlorin e6 conjugated poly(dopamine) nanospheres as PDT/PTT dual-modal therapeutic agents for enhanced cancer therapy. ACS Appl Mater Interfaces 7:8176–8187

[33] Li F, Na K (2011) Self-assembled chlorine e6 conjugated chondroitin sulfate nanodrug for photodynamic therapy. Biomacromolucules 12:1724–1730

[34] Kuznetsova NA, Gretsova NS, Derkacheva VM, Kaliya OL, Lukyanets EA (2003) Sulphonated phthalocyanines: aggregation and singlet oxygen quantum yield in aqueous solutions. J Porphyr Phthalocyanines 7:147–154

[35] Park SY, Baik HJ, Oh YT, Oh KT, Youn YS, Lee ES (2011) A smart polysaccharide/drug conjugate for photodynamic therapy. Angew Chem Int Ed 50(7):1644–1647

[36] Bae BC, Na K (2010) Self-quenching polysaccharide-based nanogels of pullulan/folate-photosensitizer conjugates for photodynamic therapy. Biomaterials 24:6325–6335